Ejection of Photoprotons from Light Elements by 45–110 Mev Bremsstrahlung

C. WHITEHEAD,* W. R. MCMURRAY,† M. J. AITKEN,‡ N. MIDDLEMAS,§ AND C. H. COLLIE
The Clarendon Laboratory, Oxford, England

(Received January 31, 1958)

Absolute differential cross sections for the production of photoprotons from carbon, lithium, and beryllium have been measured using the Oxford 110-Mev synchrotron. A proton telescope was used to select protons of energy 37 Mev, 47 Mev, 55 Mev, 63 Mev, and 78 Mev, using bremsstrahlung beams with peak energies from 40 Mev to 110 Mev. Measurements were taken at angles of 36°, 51°, 71°, 90°, 119°, and 129°. Comparison of the carbon results with the calculations of Dedrick indicate that the principal contributions to the cross sections arise from quasi-deuteron interactions. Some evidence is presented that other processes occur near threshold. Measurements of neutron-proton coincidences were made showing that this direct manifestation of the quasi-deuteron interaction occurs at these energies.

I. INTRODUCTION

EARLY experimental studies of the particles ejected from nuclei by bremsstrahlung beams in the range 20 Mev to 300 Mev showed that the yield of high-energy protons was anomalously large according to the compound nucleus theory. To explain this Levinger,[1] in 1951, proposed the quasi-deuteron model for the interaction: in this model the final high-momentum states of the emitted protons are possible because of the initial high-momentum states resulting from the proximity of a neutron and a proton in the act of mutual scattering within the nucleus. The validity of Levinger's model in the energy region between 200 and 300 Mev, has now been adequately confirmed by the detection of neutrons in coincidence with the majority of the emitted photoprotons, both by Barton and Smith at Illinois and by Wattenberg *et al.* at M.I.T.[2] On the other hand, Johansson,[3] using 65-Mev bremsstrahlung, observed few, if any, genuine neutron-proton coincidences.

However, the paucity of coincidences in the lower energy region does not necessarily indicate a breakdown of the quasi-deuteron model, for in this region there is such severe scattering of the particles while they are in the process of emerging from the nucleus that firstly, many fail to escape; and secondly, those that do get out may no longer be correlated in angle with the other partner of the initial pair and are consequently much more difficult to detect. Even if this scattering were not so serious as to prevent detection of a small but significant number of neutron-proton coincidences, the difficulty of an accurate calculation of its effect would prevent the estimation, from such experimental data, of the fraction of disintegrations attributable to the quasi-deuteron model of the process.

Numerous studies have already been made of the angular distributions of photoprotons without yielding much conclusive evidence about the nature of the interaction taking place. However, with one exception (in the 200-Mev region),[4] the data obtained have related to the yield of protons due to the whole of a bremsstrahlung spectrum, and the comparisons with theoretical predictions are necessarily ambiguous, particularly if the proton energy resolution is wide as well. The present experiments, using the 110-Mev Oxford synchrotron, were aimed at determining the angular distributions of photoprotons of selected energies ejected by the photons within a limited energy range. The predictions of the quasi-deuteron model have been calculated by Dedrick[5] in the case of carbon, and by comparison with the experimental results it is possible to judge whether the quasi-deuteron model remains valid in this energy region. Measurements on lithium and beryllium have enabled the assessment of specific nuclear structure effects. The order of magnitude of the observable proton-neutron coincidences has also been estimated.

Because of the subtraction technique employed to find the cross sections, the validity of the results leans heavily both on the accuracy of the beam normalization between different energies and on the elimination of spurious effects due to change of angular distribution of the beam with energy (and also due to random shifts in the beam direction). A system of "copper monitoring" was developed to take care of these points; this utilized the 9.7-minute β^+ activity resulting from $Cu^{63}(\gamma,n)Cu^{62}$ and this reaction was also the basis of the absolute calibration of the bremsstrahlung beam.

II. EXPERIMENTAL DETAILS

(i) General

The general lay-out is shown in Fig. 1. The accelerated electrons strike a 0.2-mm thick platinum strip inside the

* Now at CERN, Geneva, Switzerland.
† Now at NPL, Pretoria, South Africa.
‡ Now at Research Laboratory for Archaeology and the History of Art, Oxford, England.
§ Beit Trust Rhodesian Fellow.
[1] J. S. Levinger, Phys. Rev. **84**, 43 (1951).
[2] M. Q. Barton and J. H. Smith, Phys. Rev. **95**, 573 (1954); Meyers, Odian, Stein, and Wattenberg, Phys. Rev. **95**, 576 (1954); Odian, Stein, Wattenberg, Feld, and Weinstein, Phys. Rev. **102**, 837 (1956).
[3] S. A. E. Johansson, Phys. Rev. **97**, 434 (1955).
[4] J. W. Weil and B. D. McDaniel, Phys. Rev. **92**, 391 (1953).
[5] K. G. Dedrick, Phys. Rev. **100**, 58 (1955).

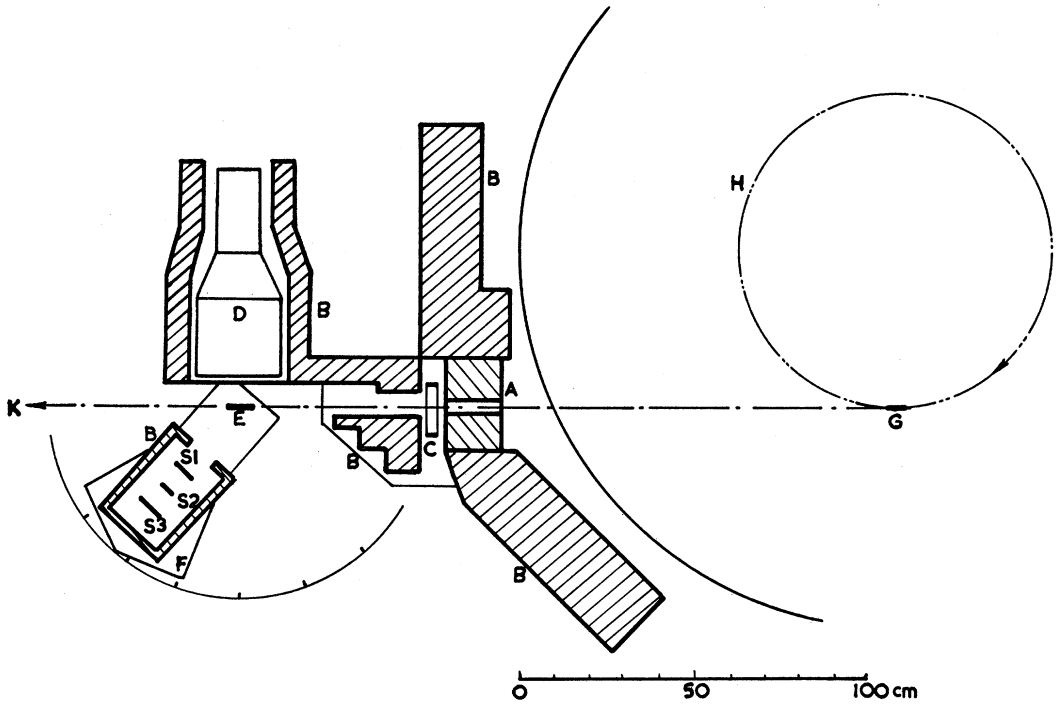

FIG. 1. General experimental layout. *A*. Lead collimation block, *B*. Lead shielding, *C*. Ionization chamber, *D*. Neutron counter, *E*. Target, *F*. Proton telescope, *G*. Synchrotron target, *H*. Synchrotron equilibrium orbit, *S*1-3 plastic scintillators.

synchrotron orbit tube and the resulting bremsstrahlung is collimated by a tapered rectangular hole in a 6-in. thick lead block; at the target position (180 cm from the platinum strip) the beam is 40 mm high and 7.8 mm wide. Immediately after collimation the beam passes through a thin air-filled ionization chamber and the charge produced in this during any proton counting period serves as a relative measure of the dose received by the target. Emitted protons were detected by a 3-scintillator coincidence-anticoincidence range measuring telescope which could be rotated about a vertical axis so as to detect protons emitted at any angle to the bremsstrahlung beam between 35° and 140°. In investigating neutron-coincidences, a large liquid scintillator was used to detect the neutrons and it was placed on the opposite side of the beam as shown.

(ii) Proton Telescope

The telescope (Fig. 2) consisted of three sheets of plastic scintillator (Pilot "B") with dimensions 5 cm $\times$10 cm, 4.5 cm$\times$12 cm, and 7 cm$\times$16 cm, respectively, each sheet being 0.3 cm thick. To ensure optimum discrimination between proton pulses and background, each scintillator was viewed from both ends by photomultipliers (Dumont type 6292), the outputs of each pair of photomultipliers being connected in parallel. The light collection was found to be further improved by recessing the scintillators into thin sheets of Perspex, optical contact being obtained using a mixture of commercial "Vaseline" and liquid paraffin. Finally, the scintillators were surrounded with cylinders of specular aluminum foil. With such optical systems the variation of light collection over the scintillators was investigated using a well collimated beam of x-rays from a 100-kv x-ray set and in no case did the light collection vary by more than $\pm 15\%$ over the area of the detectors.

The geometry was totally defined by the target volume and the second scintillator. The angular resolution was triangular with a base width of $\pm 10°$ and the effective solid angle was calculated to be 0.070 ± 0.0014 steradian. In view of the not quite perfect symmetry of the telescope with respect to the extended target the effective angles at which measurements were made differed slightly from the corresponding geometric angles. The three scintillator units operated as a coincidence-anticoincidence range measuring telescope, with resolving times of 0.2 μsec. Provision was made for the insertion of aluminum absorbers in front of the telescope and between scintillators 2 and 3.

The inherent proton range bracket width of the telescope was determined experimentally by observing the relative yields of photoprotons with different amounts of absorber between scintillators 2 and 3 and subsequent extrapolation to zero yield; good agreement was obtained with range data calculations. Measurements were made at the following mean proton energies:

Mean proton energy (Mev)	37	47	55	63	73	78
Width of proton energy bracket (Mev)	5.6	4.5	3.9	3.5	6.6	6.3

The bias levels of the three units were chosen to minimize both the random coincidence rate and the variation in proton energy bracket width due to drifts in gain and/or bias. The bias levels were set by observing the coincident pulse height distributions in each unit using an electronic gate which could be operated by either anticoincidence or triple-coincidence output pulses from the coincidence units, and the coincident spectra were displayed on a 25-channel kick-sorter.

When the bias levels had been set at their optimum values the gains of the amplifiers in the three channels were increased until gamma-rays from a weak Co^{60} source mounted on the telescope could be counted. The counting rates with these higher gains were determined accurately and subsequent three-minute determinations of these counting rates, which were made before and after each days run, yielded a 0.25% check of the telescope bracket width and also a check of the associated electronic circuitry.

Additional checks on the quality of the optical contacts were made periodically by the introduction of sources of Po^{210} and Cs^{137} close to the centres of the scintillators and the observation of the resolution of the Po^{210} α particle and Cs^{137} internal conversion electron peaks.

(iii) Neutron Counter

This counter has been described in detail by Thresher, van Zyl, Voss, and Wilson,[6] and consisted of a right cylinder 25 cm in diameter and 25 cm long filled with a liquid scintillator consisting of benzene with 4 g/liter of p terphenyl and 0.02 g/liter of diphenyl hexatriene. The scintillator was viewed at one end by a five-inch E.M.I. type VX5046 photomultiplier set in a white painted truncated cone.

The relative response of the counter over its volume was empirically adjusted for uniformity by the use of an opal disk situated between the photomultiplier and the scintillator tank. The measurements of the uniformity were made with a Sr^{90} source. The variation in response over the volume was reduced to $\pm 15\%$.

TABLE I. Neutron counter efficiency calibration.

Target	Dose (monitor units)	Protons	$n-p$ coincidences	Random coincidences
H_2O	0.614	2524	10	3.8
D_2O	0.614	3268	89	5.0
Diff.		744	79	

[6] Thresher, van Zyl, Voss, and Wilson, Rev. Sci. Instr. **26**, 1186 (1955).

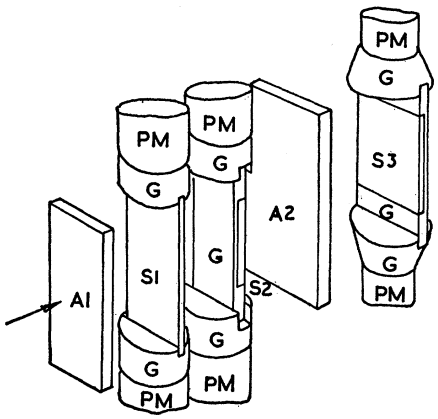

FIG. 2. Sketch of proton telescope. $A1$, 2. Aluminum absorber. G. Perspex light guides. PM. Photomultipliers. $S1$-3. Plastic scintillators.

The background due to stray synchrotron radiation was considerably reduced by means of suitably placed lead walls, but even so the final level obtained was high and consequently the minimum resolving time of 0.1 μsec of the coincidence unit (Harwell type 1036) was used in seeking neutron-proton coincidences. The random coincidence rate remained an appreciable fraction of the observed rate and was measured directly in a separate coincidence unit in which the pulses from the neutron counter were delayed by 1.0 μsec.

The position of the neutron counter with respect to the target and beam line is shown in Fig. 1; the front surface of the counter was 9 cm from the target center and in this position subtended a solid angle of 2.5 steradians.

The efficiency of the neutron counter was not readily calculable, especially in view of the large amounts of lead shielding which were in close proximity. The efficiency was more readily obtained from a measurement of neutron-proton coincidences from deuterium in a heavy water-light water difference method. In the photodisintegration of deuterium the coincident neutron and proton are emitted with defined angular correlation. In this experiment the proton telescope was set at 75° to detect protons of mean energy 37 Mev and the neutron counter was set at 90° with a bias estimated at 9 Mev. The solid angle of the neutron detector was such that in the center-of-mass system it more than encompassed the diametrically opposite solid angle of the proton telescope.

The results obtained in this measurement are listed in Table I and give a measured efficiency of 0.11 ± 0.02.

(iv) Target Assembly

To facilitate the measurement of angular distributions cylindrical symmetry is desirable in the target assembly and a target consisting of nine 3-mm diameter carbon rods was used in these measurements. The rods were placed vertically in the bremsstrahlung beam,

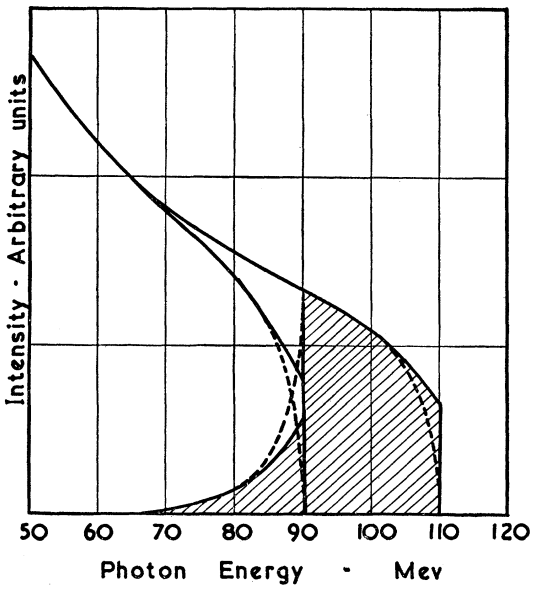

FIG. 3. 110-Mev and 90-Mev bremsstrahlung spectra normalized at 30 Mev and the difference spectrum with the Davies end correction (Bethe-Heitler spectra are shown dotted for comparison).

their height being such that they more than encompassed the vertical extent of the beam; the rods were spaced so that protons from any one rod did not traverse any part of an adjacent rod before detection. A number of rods were prepared by the U.K. Atomic Energy Authority, Harwell, from high quality carbon, and after being weighed and x-rayed nine were chosen being free from flaws or nonuniformity. The yield obtained from such a target is less than that from an extended plane target by the factor 0.47 but this loss is more than offset by the advantage of cylindrical symmetry. Measurements were also made on lithium rods with a thin protective coating of paraffin wax of known weight, and some measurements are given which were obtained using a 3-mm thick beryllium plate target.

III. BEAM MONITORING AND ABSOLUTE BEAM CALIBRATION

(i) General

The use of the photon difference method to derive the cross sections, effectively by subtraction of the normalized proton yield at one beam energy from the normalized yield at some higher beam energy, requires that the beam monitor shall be sensitive only to photons having an energy appreciably lower than the minimum beam energy used. On the other hand, if the monitor is sensitive to low-energy photons (such as results from degradation of the primary beam), then it is not a direct measure of the beam intensity. The induced β activity in copper meets both of these requirements reasonably well whereas an ionization chamber satisfies neither fully. Therefore the ionization chamber, being more convenient in operation, was used only as a run-to-run monitor and its sensitivity relative to the copper monitor was measured a number of times during each day's measurements at the various beam energies used. In fact no changes in relative sensitivity were observed during any one experimental period.

TABLE II. Copper monitoring corrections.

Bias extrapolation factor	1.15 ±0.035
Self absorption	1.00 ±0.015
Aluminum foil absorption and backscattering	1.04 ±0.01
Geometrical	2.01 ±0.005
Long-lived activities	(0.997±0.002)
$Cu^{65}(\gamma,3n)$ correction factor	0.984±0.0004
Over-all correction factor	2.36 ±0.07

The induced activity in copper is principally that due to the positron decay of the Cu^{62} which is produced by the (γ,n) reaction in Cu^{63}. The absolute measurement of the cross section of the latter reaction by Berman and Brown,[7] together with the Bethe-Heitler expression for the photon spectrum, was used to obtain an absolute calibration of the bremsstrahlung beam. Previously the beam had been calibrated by the method used by Blocker, Kenney, and Panofsky[8] for 300-Mev bremsstrahlung, but for 110-Mev bremsstrahlung this was not considered reliable to better than ±30%; in fact, according to the copper calibration the BKP method underestimated the beam intensity by 20%.

(ii) Beam Monitoring

In checking the sensitivity of the ionization chamber, a pair of copper rods 1.6 mm in diameter and 4 mm between centers were irradiated in the position normally occupied by the target. The rods covered the vertical extent of the beam and straddled the target center line; thus the induced activity in the copper rods was a good measure of the beam intensity at the target irrespective of beam shifts or changes in beam angular distribution.

A four-minute irradiation was followed by counting the activity of the rods separately and successively for 4 minutes and 6 minutes, respectively, on a 2π scintillation counter. Between 6000 and 17 000 counts (depending on the beam level) were obtained using this procedure and the break in the proton-counting schedule was only six minutes. The rods were always counted in the same order and a comparison of their activities afforded an accurate check of the beam direction.

This method was extended to determine the ionization chamber sensitivity as a function of bremsstrahlung beam energy by measuring the activity of pairs of copper rods after activation for given ionization chamber doses at beam energies between 40 Mev and

[7] A. I. Berman and K. L. Brown, Phys. Rev. **96**, 83 (1954).
[8] Blocker, Kenney, and Panofsky, Phys. Rev. **79**, 419 (1950).

TABLE III. Bremsstrahlung cross sections for photoproton ejection from carbon by 90-Mev and 110-Mev bremsstrahlung beams.

Bremsstrahlung energy Mev	Proton energy Mev	$\sigma(\theta,E_p)$ μb/Mev Q sterad 36.5°	51.4°	71.2°	90°	128.6°
110	37	1.55 ±0.03	1.67 ±0.03	1.32 ±0.03	0.792±0.013	0.292±0.015
	47	0.948±0.029	0.893±0.022	0.612±0.014	0.360±0.020	0.105±0.009
	55	0.550±0.024	0.561±0.030	0.331±0.028	0.153±0.009	0.060±0.007
	63	0.315±0.021	0.298±0.018	0.190±0.014	0.080±0.010	0.032±0.006
	73	0.142±0.009	0.128±0.007	0.063±0.005	0.026±0.003	0.003±0.003
	78	0.087±0.005	0.076±0.005	0.012±0.002	···	···
90	37	1.36 ±0.03	1.46 ±0.03	1.09 ±0.02	0.616±0.017	0.201±0.011
	47	0.666±0.022	0.700±0.018	0.440±0.015	0.243±0.011	0.070±0.007
	55	0.331±0.019	0.359±0.018	0.203±0.015	0.096±0.008	0.013±0.003
	63	0.146±0.012	0.145±0.016	0.072±0.006	0.028±0.003	0.002±0.001
	73	0.013±0.003	0.010±0.004	0.003±0.005	0.002±0.003	···
	78	0.002±0.005	0.001±0.003	···	···	···

110 Mev. By the use of these results, the yields of protons per unit ionization chamber dose were converted to yields per standard copper count.

(iii) Absolute Beam Calibration

Thin foils of natural copper of various thicknesses between 0.0005 in. and 0.040 in., width 0.12 in., and height greater than the vertical extent of the beam were irradiated separately to determine the extrapolation of the specific activity to zero foil thickness. This extrapolation was found to be independent of counter bias and in addition careful extrapolations to zero counter bias were made.

The plastic scintillator of the standard copper activity counter was covered with 0.001-in. aluminum foil and by using thinner and thicker foils the absorption factor of the 0.001-in. aluminum foil was determined.

The beam was calibrated absolutely by irradiating 0.004-in. copper foils for 10 minutes and then measuring the activity with the standard counter at a bias of 400 kev. This bias was checked frequently using a standard Cs^{137} source and the stability implied an uncertainty (other than statistical) of $<0.2\%$ in the copper counts.

As an additional check that this method had no large unforseen errors, the activity of aliquot portions of a calibrated source of P^{32} were measured by this method. All the correction factors due to extrapolation to zero source thickness, to zero bias, and for absorption were remeasured for the P^{32} electrons. The activities determined were consistent, within the experimental uncertainty of $\pm 2\%$, with the standardization (measured at Harwell on a 4π counter) which had an assessed uncertainty of $\pm 1\%$.

The counted activity of the irradiated copper rods is almost entirely the 9.7-minute half-life, 2.9-Mev positron decay of Cu^{62}. Measurements with a 0.0015-in. copper foil indicated that only $0.7\pm 0.3\%$ of the measured activity (extrapolated to zero bias) was due to longer lived activity [principally 3.3-hour half-life from the 1.2-Mev positron decay of Cu^{61} formed by the reaction $Cu^{63}(\gamma,2n)Cu^{61}$], and with the standard bias of 400 kev the contribution from this longer-lived activity was only $0.3\pm 0.2\%$.

The contribution to the Cu^{62} activity by the reaction $Cu^{65}(\gamma,3n)$ was evaluated by irradiating a separated Cu^{65} foil. Measurement of the observed activity indicated that in natural copper, 1.7% of the Cu^{62} activity (due to 110-Mev bremsstrahlung) results from this reaction and that the cross section is appreciable only between 30 and 50 Mev.

Table II lists the corrections and uncertainties applied to the activity measurements with the 0.004-in. copper foil.

The absolute uncertainty quoted for the $Cu^{63}(\gamma,n)$ cross section is $\pm 5\%$; thus the uncertainty in the absolute beam calibration obtained is $\pm 6\%$ (ignoring any additional error arising from the use of the Bethe-Heitler expression).

IV. TREATMENT OF EXPERIMENTAL DATA

The bremsstrahlung cross sections for 37-Mev photoprotons were measured at various energies for all these target materials at one or more angles. The observed yields were normalized by the copper monitoring system and the cross sections derived by the photon difference method of Katz and Cameron.[9]

In the case of proton energies above 37 Mev an abbreviated procedure was used. This was justifiable because of the relatively slow change of cross section

TABLE IV. Carbon photoproton cross sections for 96-Mev photons.

Proton energy Mev	$\sigma(\theta,E_p)$ μb/Mev sterad 36.5°	51.4°	71.2°	90°	128.6°
37	0.74±0.24	0.80±0.24	0.95±0.19	0.82±0.11	0.50±0.10
47	1.37±0.19	0.88±0.15	0.81±0.13	0.57±0.12	0.17±0.05
55	1.04±0.15	0.96±0.18	0.61±0.16	0.26±0.06	0.24±0.04
63	0.75±0.14	0.85±0.14	0.66±0.08	0.29±0.06	0.18±0.03
73	1.20±0.08	1.12±0.08	0.59±0.07	0.25±0.05	0.04±0.04
78	1.49±0.11	1.35±0.10	0.23±0.03	···	···

[9] L. Katz and A. G. W. Cameron, Can. J. Phys. **29**, 518 (1951).

TABLE V. Bremsstrahlung cross sections for 37-Mev protons from carbon.

$E_{\gamma m}$ Mev	$\sigma(\theta,E_{\gamma m})$ μb/Mev Q steradian 51.4°	71.2°	90°	118°	128.6°
110	1.67 ±0.03	1.32 ±0.027	0.792±0.013	0.380±0.022	0.292±0.015
100		1.176±0.025			
89	1.46 ±0.02	1.09 ±0.023	0.616±0.017	0.302±0.019	0.201±0.011
79		0.966±0.023			
69.6	1.110±0.032	0.844±0.022	0.440±0.009	0.175±0.014	0.134±0.022
59	0.744±0.031	0.553±0.018	0.296±0.011	0.102±0.010	0.055±0.013
53.6			0.158±0.016		
52.5				0.021±0.006	
50.1		0.180±0.008			
48.5	0.174±0.012	0.080±0.008	0.041±0.004		0.005±0.005
47.2		0.035±0.006			
45.1		0.007±0.002			

with photon energy (see Fig. 7) and, for 37-Mev protons, the cross sections deduced by each procedure were in good agreement. In the abbreviated procedure the proton yields were measured at two beam energies only: 90 and 110 Mev. The yields were then normalized to radiation doses such that the representative photon spectra were the same height at 30 Mev: these are shown in Fig. 3, the spectra being calculated from the Bethe-Heitler expression for electrons incident on platinum, using the Davies[10] end correction. The difference between the normalized yields due to the difference between the two spectra and the cross sections deduced are ascribed to photons having the mean energy of the difference spectrum, *viz.*:

$$E_{\text{mean}}=\int_{30}^{110}(\Delta n_k)k\,dk \Big/ \int_{30}^{110}(\Delta n_k)\,dk,$$

where (Δn_k) is the number of photons in the difference spectrum having energies between k and $k+dk$.

The normalization was achieved by calculating the ratio of induced copper activities due to each of the spectra normalized at 30 Mev. This ratio is

$$\int_0^{90} n_{90,k}\sigma(k)dk \Big/ \int_0^{110} n_{110,k}\sigma(k)dk,$$

and with the use of the values of the (γ,n) cross section for Cu^{63} measured by Berman and Brown[7] for $\sigma(k)$, the ratio was evaluated numerically as 1.025. Hence normalization at 30 Mev was obtained by multiplying the copper normalized yield at 90 Mev by 1.025 and subtracting from the copper normalized yield at 110 Mev.

In the case of cross sections for the production of protons of mean energies 63, 73, and 78 Mev, it is

TABLE VI. Carbon: photoproton cross sections for 37-Mev protons as a function of photon energy.

Photon energy Mev	$\sigma(\theta)$ μb/Mev sterad 51°	71°	90°	119°	129°
47	4.76±0.33	2.98±0.22	1.22±0.15	0.22±0.11	0.11±0.11
54	2.61±0.36	2.47±0.22	1.54±0.15	0.71±0.18	0.65±0.18
64	1.87±0.49	1.28±0.33	0.64±0.18	0.53±0.22	0.01±0.25
78	1.34±0.27	1.09±0.25	0.82±0.11	0.42±0.15	0.49±0.16
99	0.84±0.35	1.08±0.25	1.09±0.15	0.45±0.22	0.40±0.16

TABLE VII. Lithium: bremsstrahlung cross sections for 37-Mev protons.

$E_{\gamma m}$ Mev	$\sigma(\theta,E_{\gamma m})$ μb/Mev Q sterad 51.4°	90°
110	1.020±0.011	0.558±0.009
90	0.890±0.014	0.475±0.009
80		0.375±0.015
70	0.605±0.013	0.300±0.010
65	0.490±0.013	
60	0.366±0.011	0.212±0.008
55	0.326±0.008	
50	0.231±0.008	0.096±0.006
45	0.102±0.008	0.031±0.008
40	0.009±0.002	

[10] H. Davies (private communication).

TABLE VIII. Lithium: photoproton cross sections for 36-Mev protons.

Photon energy Mev	$\sigma(\theta,E_p)$ μb/Mev sterad 51.4°	90°
42	1.76±0.13	0.54±0.09
47	1.54±0.22	1.00±0.20
52	0.66±0.36	
54		0.60±0.11
57	0.07±0.42	
62	2.73±0.47	
64		0.55±0.11
67	1.04±0.13	
74		0.59±0.22
78	1.04±0.13	
84		0.94±0.30
99	0.49±0.15	0.23±0.10

TABLE IX. Lithium: photoproton cross sections for 96-Mev photons.

Proton energy Mev	$\sigma(\theta,E_p)$ μb/Mev sterad 51.4°	71.2°	90°	128.6°
36	0.58±0.07	0.66±0.10	0.31±0.05	0.14±0.05
55	0.51±0.05		0.34±0.03	0.03±0.03
78	0.11±0.03		0.03±0.02	

TABLE X. Beryllium: bremsstrahlung cross sections for 37-Mev photons at 90°.

$E_{\gamma m}$ Mev	$\sigma(\theta,E_{\gamma m})$ μb/Mev Q sterad
110	0.523±0.010
89	0.404±0.007
69.6	0.212±0.008
59.0	0.094±0.005
48.5	0.005±0.001

TABLE XI. Beryllium: photoproton cross sections for 39-Mev protons at 90°.

Photon energy Mev	$\sigma(\theta,E_p)$ μb/Mev sterad
47	0.29±0.10
54	0.73±0.07
64	0.83±0.10
78	0.84±0.07
99	0.48±0.10

TABLE XII. Beryllium: photoproton cross sections for 96-Mev photons at 90°.

Photon energy Mev	$\sigma(\theta,E_p)$ μb/Mev sterad
39	0.57±0.05
48	0.48±0.03
57	0.36±0.02
64	0.23±0.02

energetically impossible for some of the photons in the difference spectrum to contribute. Therefore, in computing the number of photons in the difference spectrum, the integral $\int(\Delta n_k)dk$ was cut off at the appropriate energetically defined lower limit. This limit is angle dependent and the number of photons assumed

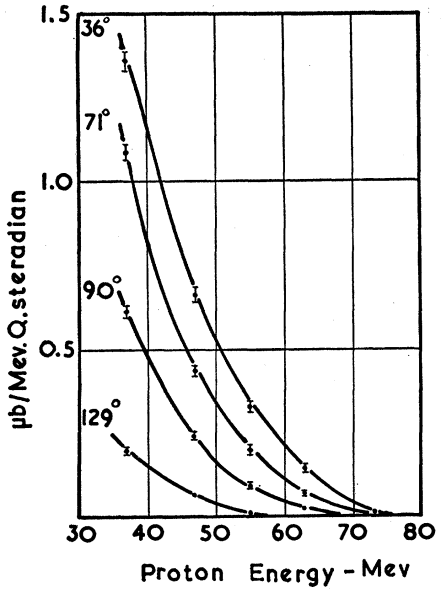

FIG. 4. Photoproton energy spectra from carbon with 90-Mev bremsstrahlung.

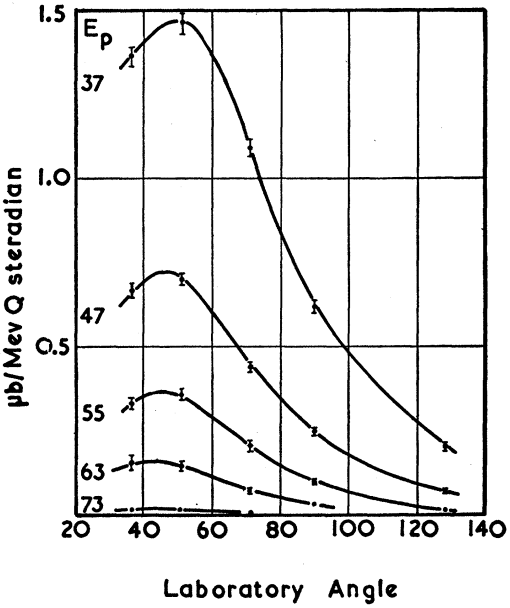

FIG. 5. Angular distributions of photoprotons from carbon with 90-Mev bremmsstrahlung.

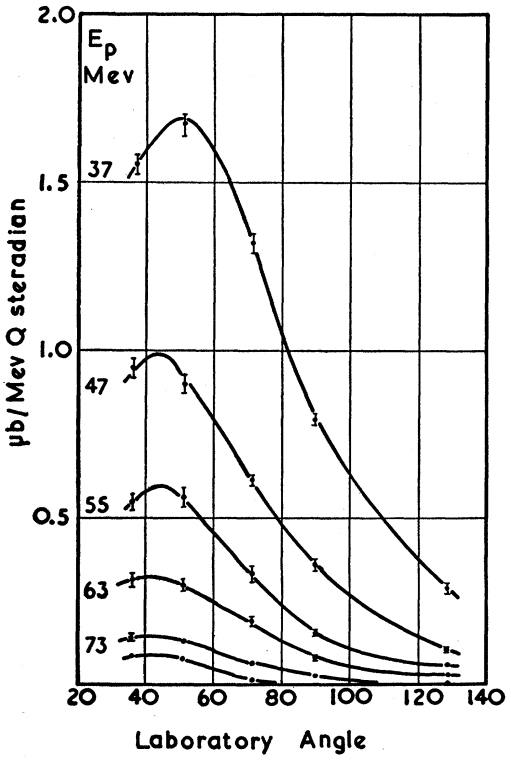

FIG. 6. Angular distributions of photoprotons from carbon with 110-Mev bremsstrahlung.

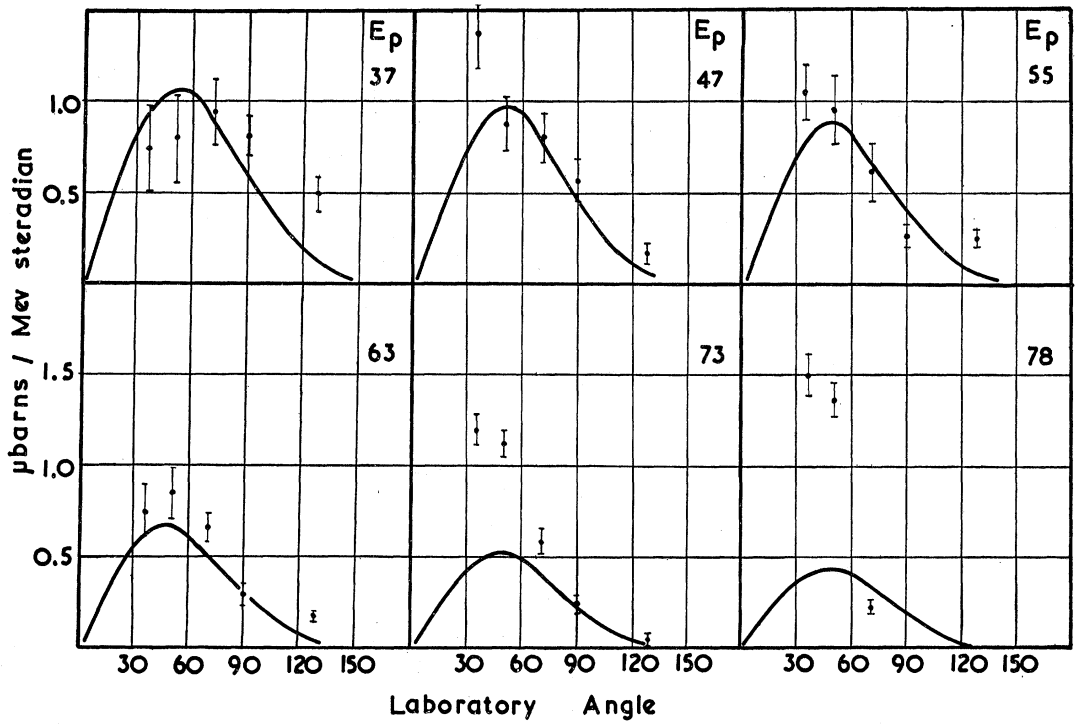

(a)

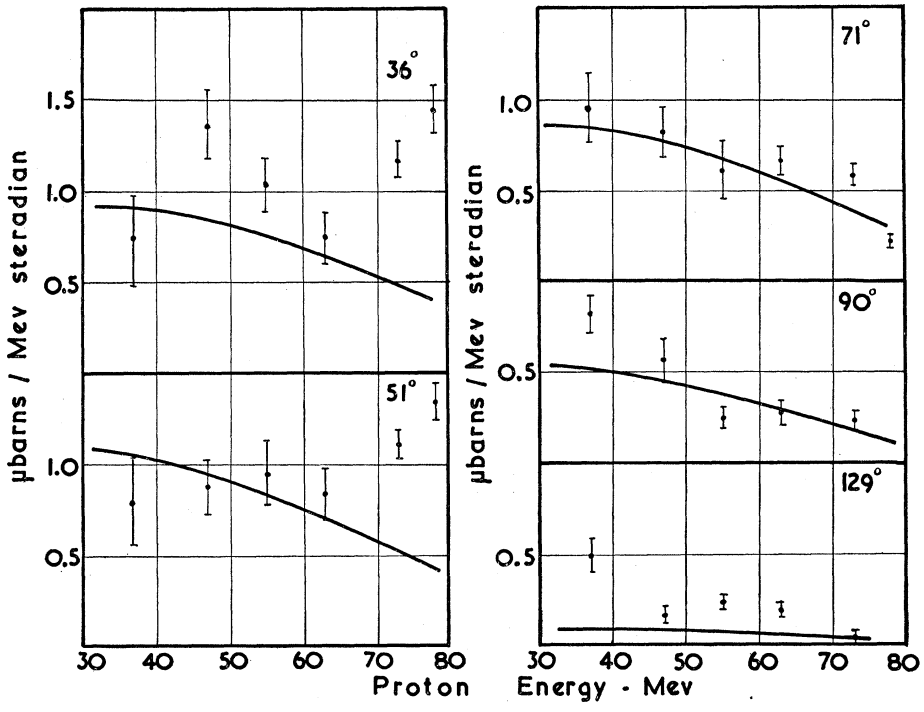

(b)

FIG. 7. Cross sections for photoproton production by 96-Mev photons on carbon. The curves shown are the quasi-deuteron calculations by Dedrick.[5]

to contribute was obtained by dividing the number of photons on the difference spectrum by factors dependent on the angle of emission of the photoprotons and lying between 1.03 and 1.06 for 63-Mev protons, between 1.60 and 2.30 for 73-Mev protons, and between 2.86 and 4.60 for 78-Mev protons.

In the foregoing it was assumed that $\sigma(k)$, the cross section for the production of Cu^{62}, fell to zero at 30 Mev as measured by Berman and Brown and remained zero at all higher energies. Since these authors did not make measurements above 35 Mev, it is not immediately justifiable to do this. However, measurements made by Jones[11] between 40 Mev and 300 Mev indicate that any high-energy tail to the cross section for the photoproduction of Cu^{62} from natural copper is small. Calculation in the limit of the experimental uncertainties of Jones' determination results in possible corrections to the calculated cross sections in the present work which never exceed 4% and in most cases are less than 2%. Such a high-energy tail would include the reaction $Cu^{65}(\gamma,3n)$ of which mention has already been made.

The results are presented in Tables III to XII and Figs. 4–15; the errors given are statistical.

V. DISCUSSION

Dedrick[5] has made a detailed application of the quasi-deuteron model of Levinger[1] to the emission of photoprotons from carbon in the energy range 50 Mev to 125 Mev. In Dedrick's model the photoprocess occurs when the energy of an incident photon is absorbed by a neutron and proton which are in the process of scattering each other inside the nucleus, and which then escape from the nuclear potential well. A wave function to describe the scattering was chosen such that it correctly describes the low-energy neutron-proton scattering and reduces to that of the deuteron ground state for the Hulthén potential. Dedrick includes in his calculation a momentum distribution having a $1/e$ value of 16 Mev, and the cross sections calculated from his work used a nuclear radius of $1.4A^{\frac{1}{3}}\times10^{-13}$ cm and a 40-Mev potential well.

Good agreement is found between these calculations and the absolute cross sections observed. This is at first sight surprising, as the Hulthén potential has been used by Schiff and by Marshall and Guth[12] to predict the photodisintegration cross section for the deuteron and at 100-Mev photon energy these latter calculations predict a value which is too small by a factor ~1.7 than that observed. By analogy, Dedrick's results might also be expected to underestimate the cross sections for carbon by the same factor. Great weight cannot be given to this analogy for although the wave function used by Dedrick does reduce to that of Schiff, Marshall, and Guth, in Dedrick's theory it describes a neutron-proton system different from that in the deuteron.

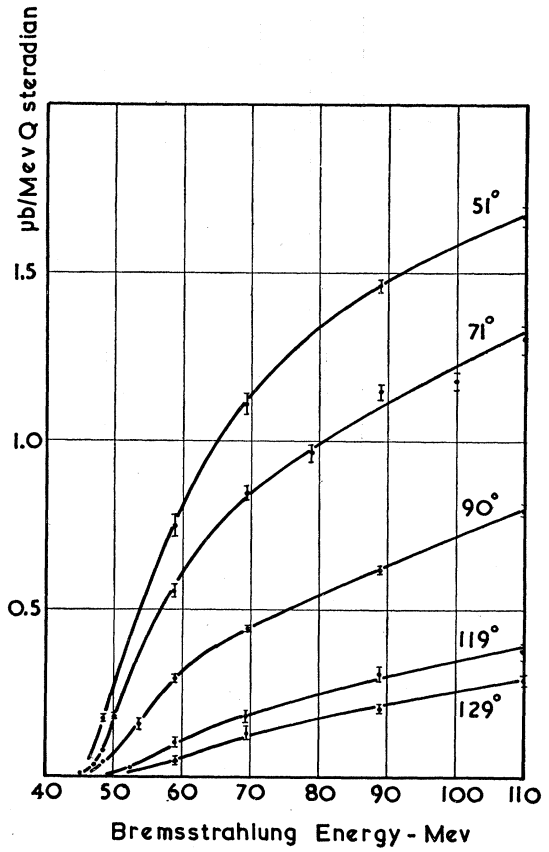

FIG. 8. Yield curves for 37-Mev photoprotons from carbon.

Two further factors must be considered: firstly, Dedrick does not take into account the effects of the scattering of the photoparticles in emerging from the nucleus, and a calculation given in the Appendix indicates that the number of observable photoparticles is reduced by the factor ~0.7 on this account. Secondly, the use of the more generally accepted value of $1.2A^{\frac{1}{3}}\times10^{-13}$ cm for the nuclear radius increases the value of Dedrick's predictions by the factor ~1.5. With all these adjustments made the cross sections observed have only half the magnitude to be expected from the quasi-deuteron interaction.

Confirmation of the validity of the quasi-deuteron model by neutron-proton coincidence observations is not necessarily feasible in this energy region. Nevertheless a brief investigation was made and the results are given in Table XIII (the results for oxygen arise incidentally from the calibration of the neutron counter efficiency). The fraction of protons accompanied by a coincident neutron has been calculated for two limiting assumptions:

(a) That there is complete directional correlation

[11] L. Jones, thesis, University of California Radiation Laboratory Report UCRL-1916 (unpublished).
[12] L. Schiff, Phys. Rev. **78**, 733 (1950); J. F. Marshall and E. Guth, *ibid.* **78**, 738 (1950).

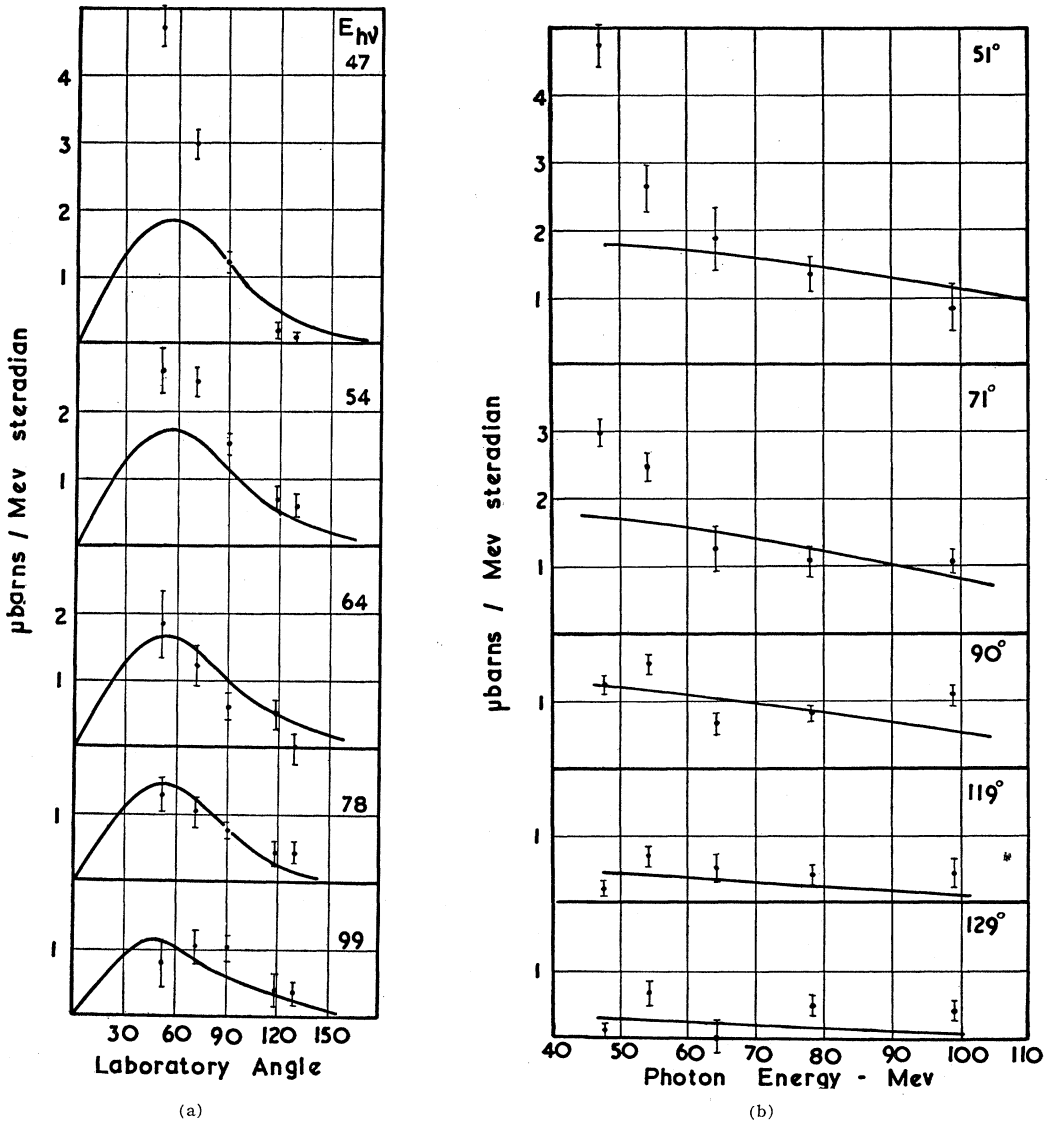

FIG. 9. Cross sections for the production of 37-Mev photoprotons from carbon. The curves shown are the quasi-deuteron calculations by Dedrick.[5]

between the proton and the neutron (carbon 0.012±0.006; oxygen 0.027±0.012).

(b) That correlation is completely absent (carbon 0.1; oxygen 0.25).

In case (a) the efficiency of detection of neutrons is just that obtained from the deuteron calibration and gives a lower limit to the yield of neutron-proton coincidences relative to the proton yield.

In case (b) the efficiency was calculated from the geometry and the *n-p* cross section in the liquid scintillator. This calculation can be done only approximately as the neutron counter is nonuniform in response over its volume; edge effects are unknown and will be complicated by the close proximity of the large amounts of lead shielding. The efficiency was calculated to be approximately 1% and on this basis an upper limit to the relative neutron-proton yield is obtained. That this limit is substantially less than 100% for carbon and oxygen strongly suggests the presence of interactions additional to the quasi-deuteron effect. This evidence is not conclusive because one member of the coincident

TABLE XIII. Neutron-proton coincidences with 110-Mev bremsstrahlung.

Target	Proton counting rate ($\theta_p=75°$, $E_p \geqslant 32$ Mev)	*n-p* coincidence counting rate ($\theta_n=90°$, $E_n>10$ Mev)	$(n+p)/p$
Carbon	2220	2.5±1.1	0.0011±0.0005
Oxygen	2524	6.2±3	0.0025±0.0011

pair may have been scattered so strongly that it has failed to emerge from the nucleus. Accordingly the remainder of this discussion will be concerned with the evidence afforded by observation of single protons.

The experimentally observed angular distributions [Figs. 7(a) and 9(a)] are in good agreement with Dedrick's predictions except when the energy of the emitted proton is close to that of the incident photon. Thus, for $h\nu=95$ Mev and $E_p=73$ Mev, for $h\nu=95$ Mev and $E_p=78$ Mev, and for $h\nu=47$ Mev and $E_p=37$ Mev, the cross sections are anomalously high in the forward direction. This cannot be an effect due to scattering of the protons during their emergence from the nucleus because such scattering, being independent of angle of emergence and involving loss of energy, would leave the angular distribution of such "threshold" protons unaltered in shape. In any case the scattering would tend to smooth out the angular distribution, and in fact it shows itself as an enhanced yield at backward angles when the proton energy is appreciably below the photon energy; the additional protons detected arise from energy degradation in the scattering process.

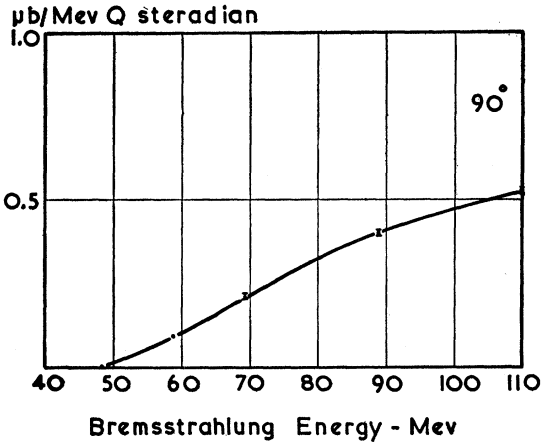

FIG. 10. Yield curve for 37-Mev photoprotons from beryllium ($\theta_{lab}=90°$).

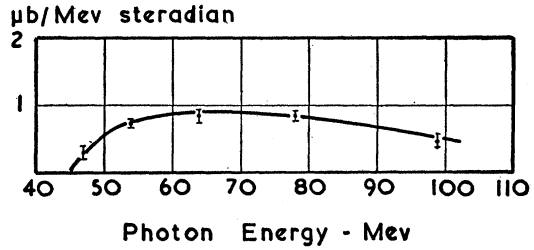

FIG. 11. Cross sections for the production of 37-Mev photoprotons from beryllium ($\theta_{lab}=90°$).

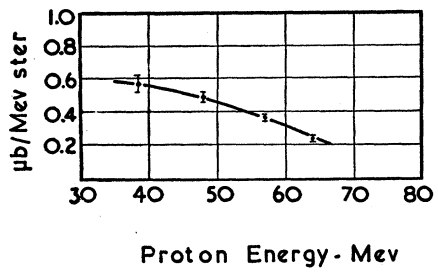

FIG. 12. Energy spectrum of photoprotons emitted from beryllium at 90° by 96-Mev photons.

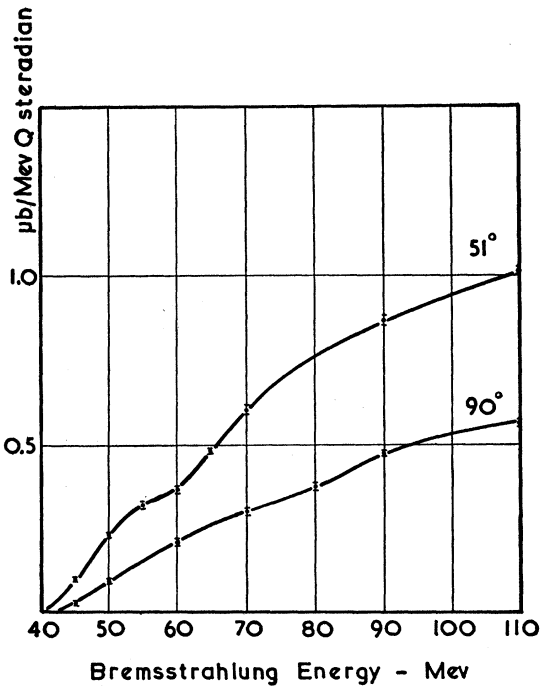

FIG. 13. Yield curves for 37-Mev photoprotons from lithium.

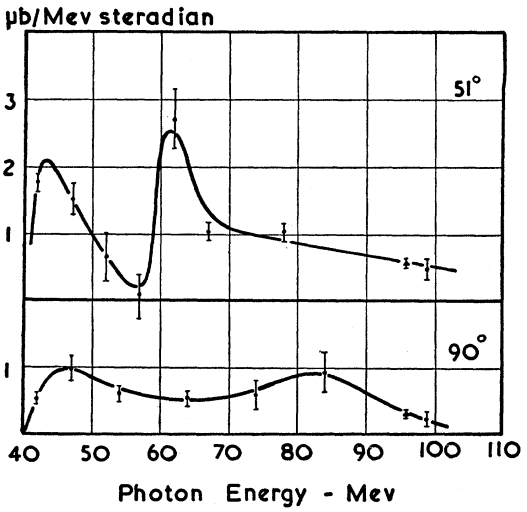

FIG. 14. Cross sections for the production of 37-Mev photoprotons from lithium.

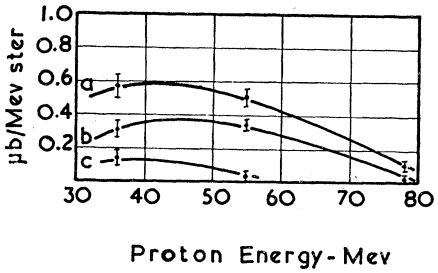

FIG. 15. Energy spectra of photoprotons from lithium produced by 96-Mev photons (a) 51°, (b) 90°, and (c) 129°.

Figure 9(b) shows the sharp peaking of the cross section just above the energetic threshold for 37-Mev protons from carbon. This sharp peaking is absent in the case of beryllium (Fig. 11), which indicates that the peaking is not a systematic experimental error. It appears that the beryllium results (Figs. 10–12), limited though they are, are in better general agreement with the quasi-deuteron theory than in carbon, where some further process appears to be contributing. In this respect the lithium results are even more striking; Fig. 13 shows a pronounced break in the excitation curve for 37-Mev protons at forward angles. As for carbon these effects near threshold appear to be strongly forward peaked. Although the relationship between photon and proton energy for these threshold protons is consistent with a direct or single nucleon interaction, the angular distributions are difficult to explain unless there is a very large quadruple interaction.

VI. CONCLUSION

Although detailed comparison between the observed results and Dedrick's predictions for carbon is made difficult by numerous experimental and theoretical uncertainties, the general trends agree remarkably well and the quasi-deuteron interaction must be accepted as a major contribution in this energy region. The large cross sections near threshold indicate contributions from other processes which are specific to particular nuclei. The occurrence of neutron-proton pairs lends further weight to the quasi-deuteron interaction and the relatively small probability of their occurrence is shown to be compatible with the estimated internal nuclear scattering.

ACKNOWLEDGMENTS

The authors wish to thank Professor Richard Wilson for useful discussions in the initial stages of this experiment and to express their gratitude to the late Professor Viscount Cherwell for extending to them the facilities of his laboratory. Acknowledgment is made to the Atomic Energy Research Establishment, Harwell, for the fabrication of the targets used and for the calibration of the P^{32} source. We are particularly indebted to Mr. A. McGill and Mr. J. McCann for their assistance in operating the synchrotron. One of the authors (C.W.) gratefully acknowledges receipt of a D.S.I.R. grant, another (W.R.M.) of a South African C.S.I.R. grant, and another (N.M.) of a fellowship from the Beit Trust.

APPENDIX

(i) Nuclear Attenuation of the Protons

The nuclear attenuation of the protons in the aluminum absorbers was calculated using the total inelastic cross section for protons in aluminum obtained from

$$\sigma_{ip}=(1-W/E)\sigma_{in},$$

where $W=Ze^2/R$ and $E=$the energy of the nucleon. σ_{in}, the total inelastic cross section for neutrons, was obtained from the work of Voss and Wilson.[13]

Corrections were calculated relative to the yield of 37-Mev protons; the correction rises to 5% for the maximum energy protons observed and this correction has been applied. The protons will also be attenuated by the plastic scintillator; but while this correction is less than 2% and has not been made, an additional $\pm 1\%$ uncertainty is placed on the correction for nuclear attenuation.

(ii) Multiple Coulomb Scattering

This was calculated from the formula given by Massey[14] but as the absorbers were appreciably larger than the scintillators the correction is less than 1%.

(iii) Nuclear Scattering of the Protons in Emerging from the Nucleus

The nuclear absorption coefficient for protons in a carbon nucleus was calculated from the total inelastic scattering cross sections of Voss and Wilson[13] for neutrons in carbon. The carbon nucleus was assumed to be spherical and it was further assumed that the photoprotons were produced uniformly throughout the nucleus. The probability of escape of the protons without scattering was calculated as a function of energy and following Weil and McDaniel[4] it was supposed that scattered protons of initial energy E would be scattered with equal probability into the energy range 20 Mev to $E-10$ Mev, the upper and lower regions being excluded by the Pauli exclusion principle.

A typical energy spectrum of photoprotons as predicted by Dedrick was then taken and the effects of internal scattering were calculated. It was found that the *shape* of the final spectrum differed only slightly

[13] R. G. P. Voss and R. Wilson, Proc. Roy. Soc. (London) **236**, 41 (1956).

[14] H. S. W. Massey, *Advances in Electronics and Electron Physics*, edited by L. Marton (Academic Press, Inc., New York, 1952), Vol. 4 p. 32.

from the original spectrum (energies below 35 Mev were not considered), the percentage decrease being independent of energy and having the value of approximately 35%. No correction was made for this effect in view of the assumptions in the calculation, but the order of magnitude of the effect has been referred to in the text.

(iv) Summary of Applied Corrections and Uncertainties

The following list gives the uncertainties in the factors used to derive the absolute cross sections:

Solid angle of telescope	1%
Efficiency of copper monitor	3.5%
Statistical uncertainty in copper monitor	1%
Cross section of $Cu^{63}(\gamma,n)Cu^{62}$ reaction	5%
Half-life of Cu^{62}	1.5%
Bremsstrahlung calculations	assumed precise
Tail of $Cu^{63}(\gamma,n)Cu^{62}$ reaction	2%
Proton telescope bracket width	3% for $E_p<60$ Mev 1.3% for $E_p>60$ Mev
Nuclear attentuation correction	1%

The over-all precision of the cross sections excluding counting statistics:

7.6% for $E_p<60$ Mev, 6.4% for $E_p>60$ Mev.

PHYSICAL REVIEW VOLUME 110, NUMBER 4 MAY 15, 1958

Natural Radioactivity of V^{50} and Ta^{180}

E. R. BAUMINGER AND S. G. COHEN
Department of Physics, Hebrew University, Jerusalem, Israel
(Received July 29, 1957; revised manuscript received February 19, 1958)

The methods of proportional counter and scintillation spectroscopy have been used to examine the possible radioactivity of the naturally occurring nuclides V^{50} and Ta^{180}. Some positive evidence is obtained that V^{50} decays by K capture to the 1.58-Mev excited state of Ti^{50} with a half-life of $(4.8\pm1.2)\times10^{14}$ yr. A search for titanium K x-rays gave negative results. For Ta^{180} a lower limit of $(2.3\pm0.7)\times10^{13}$ years was found for the half-life against decay by K capture and a lower limit of $(1.7\pm0.6)\times10^{13}$ years against beta decay.

1. INTRODUCTION

TWO naturally occurring odd-odd nuclei have been discovered during the last decade in investigations using a mass-spectrometer. They are[1] $_{23}V^{50}$ and[2] $_{73}Ta^{180}$; it may be expected that they are both radioactive.

$_{23}V^{50}$ is the central member of the isobaric triplet $Ti^{50}-V^{50}-Cr^{50}$ and should be unstable against both beta emission and electron capture. Its relative abundance is 0.25%.[3] From direct mass measurements, the energy available for the decay of V^{50} to Ti^{50} is 2.39 ± 0.13 Mev and from V^{50} to Cr^{50} is 1.18 ± 0.12 Mev.[4] The spin of V^{50} in its ground state is known to be 6.[5] A search for the radioactivity of V^{50} by other workers has so far yielded negative results.[6] In an earlier investigation in this laboratory, using Geiger counter technique, a lower limit for beta emission of 10^{12} years was found. In the present work we have searched for K x-rays of Ti with a shielded proportional counter and have examined the gamma-ray spectrum of vanadium using a scintillation spectrometer within an iron and mercury shield.

From measurements of the proton spectra in the (d,p) reaction[7] on Ti^{50}, it appears that the first excited level of Ti^{50} is at 1.58 Mev above the ground state. In accordance with the general behavior of excited states of even-even nuclei, this is almost certainly a 2+ state. Because of the high spin value of V^{50} ($I=6$), it is to be expected that V^{50} will prefer to decay with a high probability to this excited level of Ti^{50}, rather than decay by a direct transition to the 0+ ground state, despite the smaller energy difference. In this case one would expect electron capture to be accompanied by a gamma ray of 1.58 Mev. It was decided, therefore, to look particularly for a 1.58-Mev gamma ray.

$_{73}Ta^{180}$ has the very low abundance of 0.012%.[3] Its stable isobaric neighbors are $_{72}Hf^{180}$ and $_{74}W^{180}$. A short-lived isomer of Ta^{180} has been known for some years. It is produced in the reaction $Ta^{181}(\gamma,n)Ta^{180}$ and has a half-life of 8 hours.[8] Its decay scheme according to Brown *et al.*[8] is shown in Fig. 1. The average total internal conversion coefficient of the two gamma rays of 93 and 102 kev has been found to be 4.6 and the average K to L ratio is 0.15. It is to be expected that in the decay of the natural Ta^{180} the same gamma rays might be found. From the decay of the 5.5-hr isomer $_{72}Hf^{180}$,[9] a series of excited levels of Hf^{180} are known, which fit

[1] D. C. Hess, Jr., and M. G. Inghram, Phys. Rev. **76**, 1717 (1949).
[2] White, Collins, and Rourke, Phys. Rev. **97**, 566 (1955).
[3] White, Collins, and Rourke, Phys. Rev. **101**, 1786 (1956).
[4] W. Johnson, Phys. Rev. **87**, 166 (1952).
[5] Kikuchi, Sirevetz, and Cohen, Phys. Rev. **92**, 109 (1953).
[6] W. T. Leland, Phys. Rev. **76**, 1722 (1949); H. Selig, thesis, Carnegie Institute of Technology, 1954 (unpublished); J. Heintze, Z. Naturforsch. **10A**, 77 (1955).
[7] G. F. Pieper, Phys. Rev. **88**, 1299 (1952).
[8] Brown, Bendel, Shore, and Becker, Phys. Rev. **84**, 292 (1951).
[9] Mihelich, Scharff-Goldhaber, and McKeown, Phys. Rev. **94**, 794 (1954).